COBEM 2021 26th International Congress of Mechanical Engineering
November 22-26, 2021, Virtual Congress, Brazil

COB-2021-1203
PROGRESS OF ENHANCED CONDUCTIVITY FUELS USING UO2–GRAPHENE

Daniel de Souza Gomes
Nuclear and Energy Research Institute (IPEN/CNEN - SP). Av. Prof. Lineu Prestes 2242, 05508-000, São Paulo, SP, Brasil
dsgomes@ipen.br

Giovanni Laranjo de Stefani
Federal University of Rio de Janeiro (UFRJ). Av. Athos da Silveira Ramos, 149, CT - Bloco A – Cidade Universitária, 21941-909, Rio de Janeiro, RJ, Brasil
laranjogiovanni@poli.ufrj.br

Abstract. *Uranium dioxide (UO2) is the most used fuel in light water reactors. At present, a sizable cumulative experience exists regarding the use of UO_2 as a fuel. However, UO_2 has reduced thermal conductivity Experiments shown that adding a second phase with higher thermal conductivity will improve the thermal conductivity of mixed fuel. Materials such as MO and BeO dispersed in the UO_2 matrix attract the most attention. Graphene has excellent thermal conductivity and a low absorption cross-section. Metallurgic routes used in UO_2–carbon composites use the spark plasma sintering method. Thus, analyze the behavior of graphene nanoparticles dispersed in a uranium dioxide matrix, simulated with FRAPCON code. Early experiments revealed that using UO_2–10 vol.% silicon carbide improved the thermal conductivity by 30%. Graphene properties have a substantial impact on the thermal response of the fuel. In extension, carbon allotropic forms sintered with UO_2 are potential options like UO_2-diamond and UO_2-nanotubes.*

Keywords: *Graphene, Spark Plasma Sintering, FRAPCON, SERPENT, Accident-Tolerant Fuel*

1. INTRODUCTION

UO_2 fuel has a low thermal conductivity, which reduces upon irradiation. A result of the poor thermal transport of UO_2 is a large temperature gradient within the fuel pellet, which generates a higher centerline temperature and proportional thermal stress. The elevated fuel temperature is unsafe, creating strains, swelling, and releasing more fission gases. Thus, it induces the pellet cladding mechanical interaction, which speeds up the fuel cracking process combined with fuel relocation. Accident-tolerant fuel (ATF) requirements may improve the thermal conductivity, chemical stability, high oxidation resistance, and low manufacturing cost (Terrani, 2018). Irradiation induced densification of UO_2 sintered, below 10 MWd kgU^{-1}. As a result, it increases linear heat generation, enhances local neutron flux, and reduces the gap conductance because of the size reduction. Deficient heat transport combined with fuel thermal expansion and irradiation causes cracking of the UO_2 pellets.

In the past 60 years, power reactors have used uranium dioxide as a nuclear fuel for pressurized water reactors (PWRs). However, after the Fukushima Daiichi disaster, the ATF plan and advanced fuel campaign researched innovative options. The proposal described in this study comprises a mix of graphene nanosheets with a high thermal conductivity dispersed in a UO2 matrix (Yao et al., 2018). This concept uses the addition of a second-phase material with enhanced thermal conductivity and a lower neutron cross-section. The UO_2–graphene composite has little impact on moderate neutron flux. The manufacturing route used for UO_2 pellets comprises the following steps: first, the powders are mixed and milled, followed by initial compaction, granulation, final compaction, and sintering for 4–10 h at 1600°C (Gomes and Silva, 2019). However, UO_2–graphene consolidation uses the spark plasma sintering (SPS) method (Cartas et al., 2015). The SPS had shown excellent results for UO_2-SiC, UO_2-Mo, UO_2-BeO produced on a laboratory scale (Li et al., 2020).

Aiming at a high thermal conductivity of the ceramic fuel can add a second phase, which contains materials with a higher thermal conductivity using SiC, BeO, and carbon nanomaterials (Hilty and Tonks, 2020). UO_2 doped with beryllium oxide shows a high conductivity. UO_2–BeO with 9.6-vol.% BeO increases the thermal conductivity by 10% (Gomes et al., 2019). The metallic fuel uranium molybdenum (U–10-vol.% Mo) has a high thermal conductivity of 12 W. m^{-1} K^{-1} at room temperature and poor corrosion resistance in contact with water (Finkeldei et al., 2019). Thus, the molybdenum phase enhances the thermal conductivity, but U–Mo produces bubbles under irradiation (Hu et al., 2015). Therefore, molybdenum has an expressive neutron absorption cross-section of 14 barns for a moderate neutron flux.

Mixed ceramics with nanoscale carbon have attracted interest for experiments combining UO_2 and nanocarbons, such as silicon carbide (SiC) and carbon allotropes dispersed in the UO_2 matrix (Yeo et al., 2013). Researchers using UO_2 powder mixed with SiC particles of less than 16.9 μm and sintered by the SPS method at 1350°C–1450°C for 5 min.

Resulting in enhanced thermal conductivity in a 30% increase in thermal conductivity (Tulenko and Subash, 2016). However, a UO_2–SiC 10-vol% pellet exhibits a 62% improvement in heat transport compared with UO_2

Currently, there is growing interest in adding carbon allotropes, as the second phase, into the UO_2 matrix, such as carbon nanotubes (CNTs) and SiC (Gomes et al., 2017). Branches of graphene (5 vol.%) have enhanced thermal conductivity by 29.7% relative to pure UO_2. However, under irradiation, the addition of SiC resulted in enhanced cracking, and the UO_2–diamond showed a disrupted microstructure (Tulenko and Subhash, 2016). As a result, the composite fuel formed by UO_2–graphene can increase the thermal conductivity, power density, and maximum allowable fuel burnup (Lee et al., 2011). Another option incorporates a small amount of Cr_2O_3 and Al_2O_3 into UO_2, which enlarges the fuel grain size, increases fuel density, improves the retention of fission gases, and has an excellent viscoelastic response (Arborelius et al., 2006). Table 1 summarizes some properties of ceramic fuels and carbon allotropes.

Table 1. Physical properties of pure UO_2 and carbon compounds used as dopants.

Physical Properties	**UO_2**	**BeO**	**Graphene**	**CNTs**	**SiC**
Melting Point, °C	2880	2530	3674	3674	2730
Density, g cm^{-3} (1)	10.960	3.02	2.670	2.600	3.21
Thermal Conductivity, W m^{-1} $°C^{-1}$ (1)	8.68	250	2500 ± 50%	3000 ± 50%	275 ± 10%
Thermal Expansion, 10^{-6} $°C^{-1}$ (1)	9.76	7.4	−4.8	4.25 ± 20%	3.5 ± 25%
Specific Heat Capacity, J kg^{-1} $°C^{-1}$ (1)	235	750	950	425	655 ± 5%
Elastic Modulus, GPa (1)	192	331	1022	1055	418 ± 12

(1) measured at 25°C and 0.1 MPa

1.1 Computational tools

The SERPENT package is a continuous-energy Monte Carlo code dedicated to simulation reactor physics calculations. Since 2004, the serpent has gained global recognition supported by the Technical Research Centre of Finland (Leppänen et al., 2015). Neutron transport simulation of full-core 3D models used the design control documentation of Westinghouse. SERPENT calculates the effective reactivity coefficient critical for nuclear reactor operations, guaranteeing safety and stability. In this study, the thermal neutron flux distribution of the PWR reactor employed the SERPENT code. The core analysis of the AP 1000 reactivity of UO_2–graphene covered the criticality, peak power factor, reactivity, critical boron concentration time, and total outage reactivity during burn cycles.

The fuel rod performance analysis for LWRs used the FRAPCON code developed by the Pacific Northwest National Laboratory. The U.S. National Regulatory Commission (USNRC) suggests using the FRAPCON code for licensing and auditing nuclear reactors in the United States (Geelhood et al., 2015). FRAPCON predicts UO_2 and (U–Pu)O_2 or mixed oxide, UO_2–10-vol% Gd_2O_3, and zirconium alloys (zircaloys) as cladding. Another fuel rod or coolant requires a complex code upgrade, adding new physical models and material properties. For 2020, it upgraded FRAPCON to the latest FAST version (Porter and Geelhood, 2018). FAST can simulate regular and transient operation in the only merged system, extending cladding options to ferritic alloys. However, FRAPCON underwent several changes to account for the UO2–graphene properties to analyze steady-state fuel performance in a PWR core.

2. UO_2–GRAPHENE PHYSICAL PROPERTIES

The physical properties of graphene and its derivatives depend on the material type, such as graphene monolayers, reduced graphene oxide, and graphene nanosheets. In addition, each sheet has a one-atom-thick carbon synthesized in bulk using various chemical techniques. Although the significant importance of thermal properties, measured using several methods, such as spectroscopy and molecular dynamics. The physical properties of graphene outperform those of CNTs using spectroscopy, measuring thermal properties and compressive and tensile strains.

Increasing the thermal conductivity of nuclear fuel would improve nuclear safety during regular operation and under accident scenarios. ATF program made extensive efforts to find more tolerant fuel systems, using the addition of high thermal conductivity compounds as the second phase, mixed with UO_2. Uranium monocarbide (UC) or uranium–plutonium carbide (U–Pu)C are fast reactor fuels that exhibit complex preparation and sintering routes. UC has a high uranium density, good irradiation stability, and exceptionally high thermal conductivity. Monocrystalline graphite has a mass density of 2.26 g cm^{-3}, a high thermal conductivity of 2000 W m^{-1} K^{-1} at 25°C, and a melting point of 4227°C. In contrast, diamond shows a mass density of 3.515 g cm^{-3}, a high thermal conductivity of 2200 W m^{-1} K^{-1}, a specific heat capacity of 520 J kg^{-1} K^{-1}, and an elastic modulus of 1143 GPa at 25°C.

The innovative (UO_2–5 vol.% diamond) comprises a nuclear fuel with an enhanced thermal conductivity that should reduce fission gas release (FGR) compared with pure UO_2. However, diamond powder of several micro sizes (3, 12, and 25 μm) and size (0.25 μm) mixing to UO_2 powder and sintered using SPS at 1300°C–1600°C with a hold time of 5 min.

Allotropic forms of carbon atoms show several crystal structures composed of distinct types of orbital hybridization, which reveal original properties (Acik and Chabal, 2011). For example, the cubic shape of diamond is a sp^3 hybrid state of carbon, and graphite has sp^2-hybridized carbon (Terrones et al., 2010).

Nanomaterials involve particles of 1–100 nm with structures of up to three dimensions (3-D). Graphite is an infinite sheet of a honeycomb lattice structure that facilitates weak interlayer interaction. The molecular arrangement of graphite is trigonal planar with a covalent bond. Graphite comprises hundreds of thousands of layers of stacked graphene. A Fullerene is an allotropic form of carbon that is zero-dimensional. CNTs are one-dimensional, graphene nanoplatelets are two-dimensional, and diamond and graphite are 3-D materials (Akinwande et al., 2017). Investigations have found new geometric forms, such as ball shapes for fullerenes, planar sheets for graphene, and cylindrical models for CNTs (Bhushan et al., 2014). Nanotube and graphene are hexagonal packed structure sp^2 hybrids. However, amorphous carbon is an allotropic form of carbon that does not exhibit any crystalline structure.

There are many methods to get graphene, such as mechanical exfoliation, chemical reduction of graphene oxide, chemical vapor deposition, and thermal decomposition on SiC. The mechanical exfoliation of graphite was the first method used to synthesize graphene. It comprises the Scotch Tape method, which uses Scotch Tape on graphite, and then transfers by pressing (Kumar et al., 2021). This technique has poor scalability for industrial production substituted by chemical exfoliations that use the dispersion of graphite powder in a solvent followed by sonication. However, the sintering of the nanocomposite employs the SPS technique because the conventional route forms significant porosity.

The traditional sintering route used for UO_2 involves a liquid phase to improve the sintering rate. Despite this, the sintering technique of UO_2 without external pressure has several drawbacks, such as long sintering periods over ten hours at 1700°C, fuel disintegration at elevated temperatures, and significant grain growth. However, field-assisted sintering techniques have provided a remarkable capacity for consolidation, which permits a brief sintering time of 5 min and lower temperature using the SPS technique (Ironman et al., 2017).

In the SPS machine, the UO_2–graphene heated powder sintered under a pressure of 40 MPa and subjected to direct pulsing at a low voltage (5–15 V) with a current of approximately 10 kA. In SPS, it can achieve a heat transfer rate from 50 to 400 K min^{-1}, limiting grain growth and improving mechanical properties. Because the SPS route uses short sintering times, it is ideal for fuel composites and nanomaterials.

2.1 Neutron assessment of graphene composite fuel

Mixed fuel experiments show that volume additions of graphene between 5% and 10% are appropriate. The results show that increased enrichment is necessary to maintain the overall reactivity provided by the fuel lattice for the entire fuel cycle. The neutron flux simulation used the SERPENT code, comprises a 3-D system widely used in lattice physics. Besides, the neutron flux features of the UO_2–graphene fuel during the irradiation cycle decreased the ^{239}Pu buildup. Figure 1 displays the effective multiplication factor (k_{eff}) of the PWR 17 × 17 AP1000 reactor using UO_2 and UO_2–graphene.

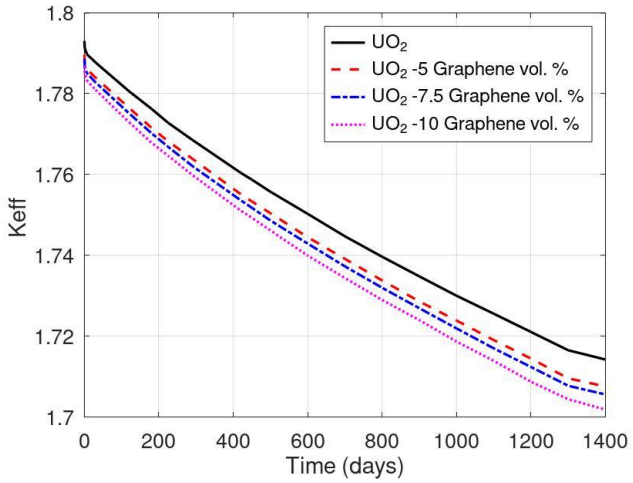

Figure 1. Multiplication factor k_{eff} versus effective power days for UO_2 with graphene (5, 7.5, and 10 vol.%)

In addition, the reactivity coefficient of the composite fuel is noteworthy in that increasing the graphene volume fraction leads to less negative reactivity feedback. The AP1000 is a PWR reactor that includes a passive core cooling system with two cooling loops to produce a net power output of 1117 MWe. The refueling interval is 18 months, which is equal to the close power of the burn cycle.

Currently, AP1000 technology scale up the AP1000 power generation capacity and the Chinese version CAP 1400 achieves 1500 MWe. The AP1000 PWR uses a 17 × 17 configuration for fuel assemblies, with U^{235} enrichment (assumed to be 4.45%), ZIRLO, a (Zr–1Nb) alloy cladding thickness of 0.57 mm, and a pellet thickness radius of 4.096 mm. The internal pressure is 15.5 MPa, the fuel pitch is 12.5984 mm, and the active fuel length reaches 4.27 m, typical of PWR reactors. For composite fuel UO_2 with 5-vol.% graphene, the enrichment is 4.68%, and for 10-vol.% graphene, U^{235} enrichment is 4.94%.

2.2 Thermal properties

The thermal conductivity of carbon allotropes spans a considerable range. Amorphous carbon has the lowest (0.01 W m^{-1} K^{-1}). At room temperature 293.15 K, the thermal conductivity of diamond and graphene exceeds 2000 W m^{-1} K^{-1}, and CNTs are between 3000 and 3500 W m^{-1} K^{-1}. The thermal conductivity of the carbon allotropic form exhibits notable variability. The uncertainty in the thermal conductivity measurements of suspended graphene was 4840–5300 W m^{-1} K^{-1}, while that calculated by the Green–Kubo method was 2903 ± 93 W m^{-1} K^{-1} for pristine graphene. In addition, the out-of-plane phonon mode contribution reached 1202 ± 32 W m^{-1} K^{-1}, showing a strong dependence on size width. Figure 2 shows the thermal conductivity at low temperatures of the allotropic forms of a few carbons.

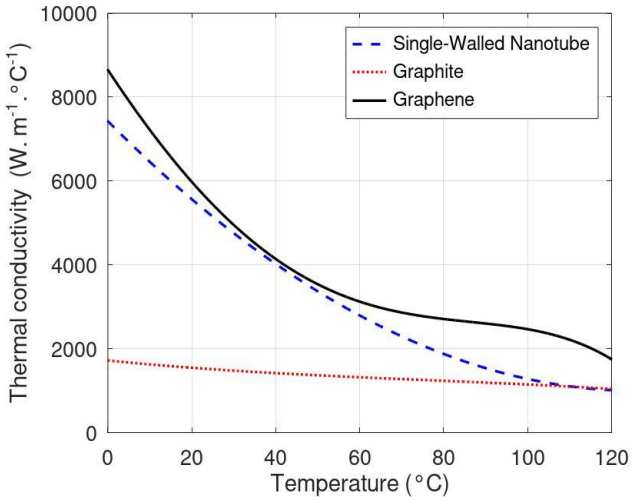

Figure 2. Thermal conductivity of single-walled CNT, graphite monolayer, and graphene.

Graphene has a thermal conductivity of 5000 ± 250 W m^{-1} K^{-1} and has a high heat capacity. However, the transport of thermal energy depends on the vibration of the atoms. Ultrahigh thermal conductivity makes graphene the most promising additive for enhancing the thermal conductivity of composite fuels. The repetitive hexagonal structure of graphene improves thermal conductivity and is one of the most robust materials discovered to date. For ATF, boost experiments using UO_2 blended with carbon allotropes, such as graphene, CNTs, and diamond.

Researchers have conducted many theoretical investigations to predict the phonon and thermal properties of graphite graphene and CNTs. These models employ different methods, such as density functional theory, Boltzmann transport models, and micro-Raman spectroscopy. Numerical simulation approaches used to calculate the thermal conductivity are functions of the temperature profiles coupled with the size and shape of the particles. Thus, there is a consensus that thermal energy transference depends on the phonon transport mechanism, combined with the reduced effect of electrons. Therefore, the synthesis route used to obtain graphene has a substantial weight in terms of the magnitude of the heat transfer. However, researchers have reported a considerable uncertainty between flakes, powder, and graphene film, which depends on synthesis methods, sintering parameters, aspect ratio, and impurity levels. In addition, the thermal conductivity increases with length up to the mean free path of phonons, showing a variation that reduces the conductivity with the number of graphene layers.

Carbon allotropes exhibit physical properties that depend on manufacturing, purity, lattice defects, and atomic structures. UO_2–graphene has an expressive mechanical performance that improves the elastic modulus, toughness, and hardness. Graphene shows a low density combined with a higher melting point compared with UO_2. Graphite and graphene have a high heat capacity, which increases the stored energy of the fuel. Hasselman and Johnson's formulation represents a fitting model for predicting the thermal properties of composites. This model uses the volume fraction of each component of the mixture, analyzing the effect of the interfacial thermal conductivity combined with the reinforcement fiber parameter defined in each particulate composite. Figure 3 shows the thermal conductivity of the composite fuel with UO_2–(5–10)-vol.% graphene and pure UO_2.

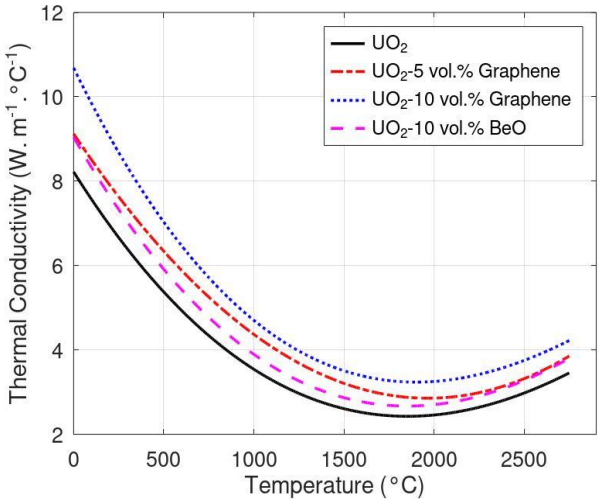

Figure 3. Thermal conductivity of UO_2 and (UO_2–5 vol.% and UO_2–10vol.% graphene).

Graphene has a negative coefficient of thermal expansion (CTE) as water, meaning that the material contracts or shrinks. Experimentally, the CTE of graphene is -7×10^{-6} °C^{-1} at 25°C, and its magnitude decreases with increasing temperature. Lattice dynamic analysis reveals a combination of phonon vibration and elongation effects, producing a negative thermal expansion. The CTE of graphene reaches -8×10^{-6} °C^{-1} when measured through Raman spectroscopy, but other measurements show graphene has a positive coefficient at more than 327°C. Figure 4 displays the thermal expansion coefficients of graphene, SiC, and UO_2. However, SiC exhibits anisotropic behavior, and many polytypes are comparable to graphene.

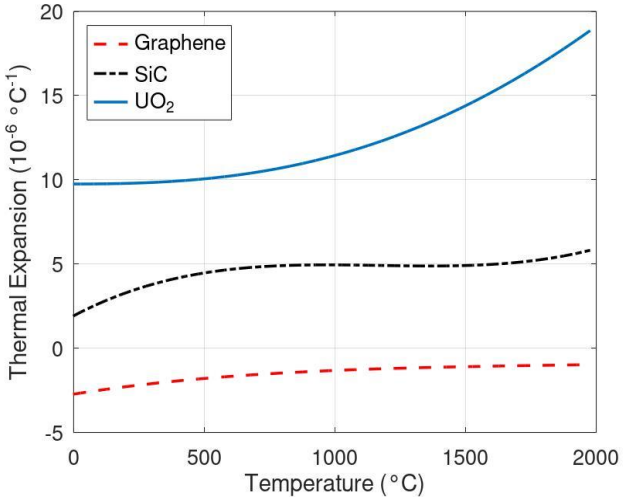

Figure 4. Thermal expansion coefficients of pure graphene, silicon carbide, and uranium dioxide.

The theoretical model used to study the thermodynamic properties of graphene sheets uses density functional perturbation theory. The specific heat of graphene reaches 600 J kg^{-1} °C^{-1} near room temperature, 20°C. Although phonon frequencies are crucial for using dynamic simulation cases, the experimental databases are comparable with the computed thermodynamic properties.

The heat capacity of UO_2–graphene is a combination of volume fractions multiplied by the heat capacity of each component. The same model produced a valued numeric fit to UO_2–SiC, UO_2–CNTs, and UO_2–diamond (Cartas et al., 2015). In comparison, other allotropic forms, such as graphite, have a heat capacity between 690 and 720 J kg^{-1} °C^{-1} at 20°C, while that of the diamond is approximately 502–519 J kg^{-1} °C^{-1} and that of UO_2 is 220 J kg^{-1} °C^{-1}. Figure 5 shows the heat capacities of graphene, diamond, graphite, and UO_2.

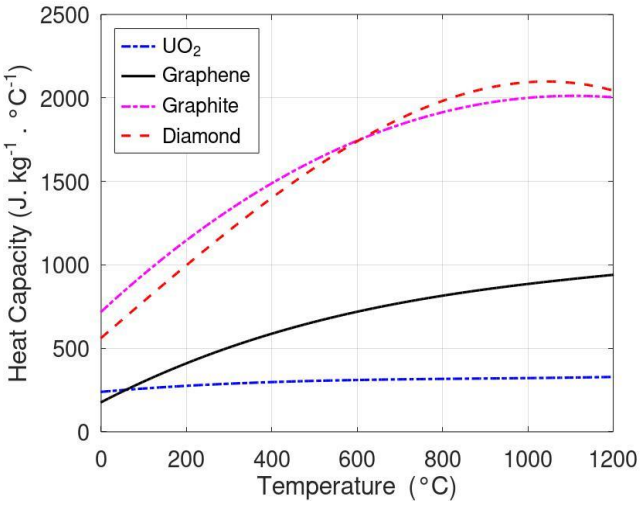

Figure 5. The heat capacity of UO_2 and carbon allotrope forms, such as graphene, graphite, and diamond.

2.3 Mechanical properties

Several methods exist to measure the mechanical response of graphene monolayers based on molecular simulations. Besides, mechanical properties result from a carbon bond network with an elastic modulus of over 1000 ± 100 GPa, the shear modulus of 412 MPa, and the fracture strength of 130 ± 10 GPa. An elastic modulus of over 1000 ± 100 GPa, shear modulus of 412 MPa, and fracture strength of 130 ± 10 GPa. The Young's modulus of graphene can vary between 0.5 and 2 TPa. The Poisson ratio of graphene is 0.16, which corresponds to graphite in the basal plane. However, because of anisotropic behavior, found values between 0.17 and 0.186. Incorporating graphene into the UO2 matrix increases the mechanical resistance of the fuel pellets against cracking propagation, reducing by the high thermal conductivity. Defect-free monolayer graphene has excellent mechanical properties, such as a high elastic modulus of 1100 GPa and a tensile strength of 130 ± 0.1 GPa, which reveals a reduced strain under stress. Figure 6 displays the elastic modulus of pure UO_2 and the composite fuel UO_2–graphene containing 5 and 10 vol.%.

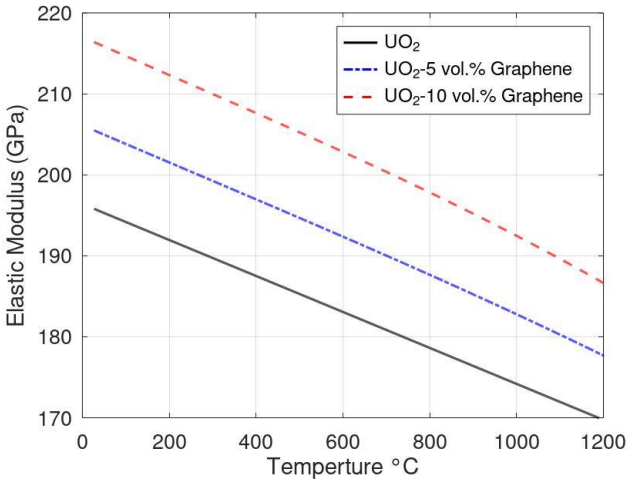

Figure 6. Elastic modulus of UO_2 pure and composite fuel (UO_2–5 vol.% and UO_2–10 vol.% graphene)

3. SIMULATION RESULTS

The simulation process used a steady-state operation test based on single-rod fuel performance using the licensing code FRAPCON. It got the material property models used for standard UO2 from the Materials Property (MATPRO) package adopted by the USNRC (Hagrman and Reymann, 1979). The base irradiation of the full-length rod comprised six irradiation cycles that corresponding to 1400 days. The AP1000 reactor core 17 × 17 typical assemblies with 157 fuel assemblies, 264 fuel rods, 24 control rod guide tubes, and a neutron monitor guide tube.

Fuel assemblies show three different regions with enrichment of 2.35%, 3.40%, and 4.45% for simulations with 4.45% enrichment. Table 2 lists the nuclear fuel reactor parameters.

Table 2. Parameters of PWR AP1000 17 × 17

Nuclear Reactor Characteristic	Values
Fuel Pin Array	17 × 17
Fuel Theoretical Density, %	95.5
Fuel Roughness, mm	1.20
Pellet Outer Diameter, mm	9.50
Pellet Length, mm	9.83
Cladding Outer Diameter, mm	10.75
Cladding Roughness, mm	0.7844
Cladding Thickness, mm	0.0571
Active Stack Length, mm	365.76
Pitch, mm	12.54
Enrichment, ^{235}U, %	4.45
Plenum Length, mm	141.93
System Pressure Nominal, MPa	15.51
Water Inlet Temperature, °C	301.67
Gap Gas Pressure, MPa	2.00
Coolant Mass Flux, kg s^{-1} m^{-2}	3539.76

The reactor core of AP1000 uses a robust fuel assembly design containing 95,974.7 kg of UO_2 sintered with a density of 10.96 g cm^{-3}, distributed in 41,448 fuel rods, with each rod having an active length of 4.27 m. Typical configurations operate in three regions of U^{235} enrichment: 2.35, 3.40, and 4.95 wt%. Thus, the AP1000 reactor under normal conditions should operate at an average linear heat rate of 18.7 kW m^{-1} and an average fuel power of 109.7 MW m^{-3}. The fuel pellet temperature distribution shows a maximum value at the pellet centerline, below UO_2 melt temperature, decreasing in the outer surface direction. Figure 7 shows that the temperature of UO_2–10-vol.% graphene is lower than that of pure UO_2 because of the enhanced conductivity of the graphene additions.

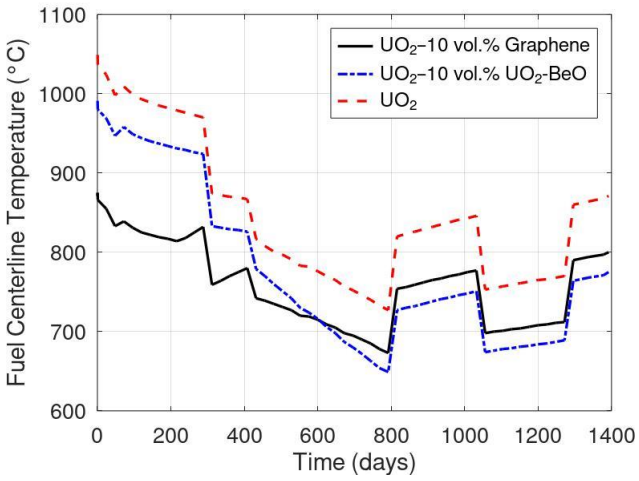

Figure 7. Fuel centerline temperature of fuels analyzed

The safety margins are physical barriers to avoid radioactive isotope releasing into the environment. Under safety analysis, there are maximum limits for fuel temperature, fuel enthalpy, clad temperature, clad strain, and clad oxidation.

Graphene addition improves the thermal conductivity of mixed fuel and reduces the FGR rate, fuel swelling, fuel damage, and thermal creep effects. Reducing the fuel centerline temperatures mitigates the risk of uranium dioxide melting at approximately 2804°C unirradiated and decreasing by 14°C per 10,000 MWd kgU^{-1}.

MATPRO is the primary source of material property and behavioral models in the FRAPCON code and FAST version. Several physical models contain uncertainties, such as fuel pellet relocation, densification, melting, swelling, and heat transport capacity. The radial power distribution employs the Forsberg–Massih model for FGR. The radial distribution of pellet temperature for the UO_2 pellet without graphene addition reached 815°C.

The lower curve shows for UO_2–10 vol.% graphene, the temperature was lower, reaching 645°C. Figure 8 displays the internal pellet temperature in the radial direction for UO_2–BeO.

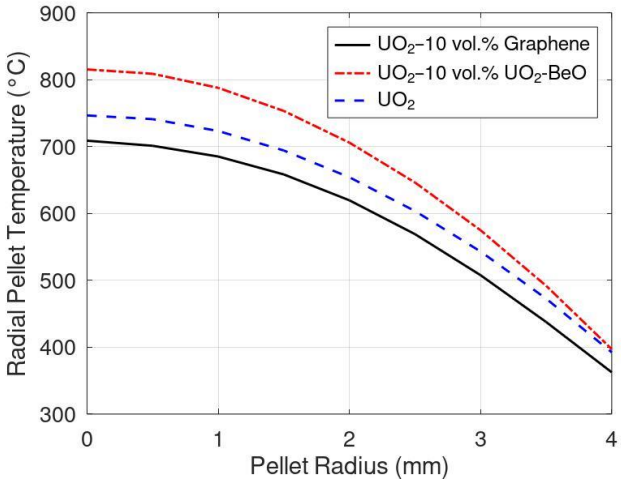

Figure 8. Radial pellet temperature of UO_2–BeO, UO_2, and UO_2–graphene

The energy stored in the fuel integrates the steady-state temperature distributions in the fuel pellet and cladding. In addition, a lower thermal conductivity produces less stored energy, whereas a high thermal conductivity implies that fuel will store more energy. Figure 9 displays the stored fuel energy of the analyzed fuels. In addition, it considers the temperature variation of the thermal conductivities and the radial variation of fission power in the pellet.

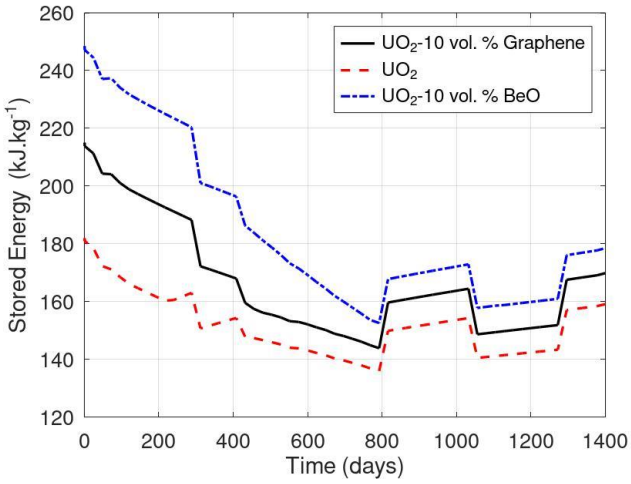

Figure 9. Fuel stored energy for UO_2, UO_2–graphene, and UO_2–BeO

The potential benefits of UO_2–graphene composite pellets include enhanced thermal transport capacity with a lower neutron absorption cross-section of graphene. The SPS method is more rapid, spent a few minutes, reaching higher densities at lower temperatures while minimizing grain growth. Composite pellets show a slight reduction in grain size (12 ± 2 µm), while pure UO_2 is 15 ± 5 µm. A small grain size promotes the FGR rate. SPS achieved a fuel density of 10.79 g cm^{-3} for UO_2–graphene. Besides, the mixed pellets have a reduced cracking process because of their higher mechanical strength and reduced thermal expansion. The simulation shows results comparable to those reported for fuels based on carbon compounds.

4. CONCLUSION

Results from simulation show reduced fuel temperature, the centerline of pellet UO2 exhibit 800 C and UO2-graphene reach 700 C lower temperature than UO2-BeO. Theoretically, the fission gas release model shows temperature dependence. Besides, a lower gradient produces decreased gaseous fission products. Under fission, composite fuel behavior could be like an amorphous carbon compound but needs an extensive experimental phase. Under irradiation,

still had brief experiments to predict effects. The volume of graphene produces benefits increasing linearly with increasing thermal conductivity in terms of reduced fuel center temperature. FRAPCON performance code show a lower radial fuel rod temperature and peak cladding temperature compared to UO_2. Possibly, the safety margins will suffer improvements in any situation. Besides, the chemical compatibility of innovative fuel is extensive without restriction on any cladding material. In principle, graphene avoids graphitization as UO_2-diamond and shows higher conductivity than UO_2-SiC. An important feature, the fuel needs more enrichment to maintain the overall reactivity provided by the fuel lattice for the entire fuel cycle. In extension, the neutron flux features of the UO_2–graphene fuel during the irradiation cycle reduces Pu^{239} production.

ATF concepts involve UO_2 composite fuels that contain secondary phases with higher thermal conductivity, such as CNTs, UO_2-diamond, and UO_2-SiC. This study used UO_2-graphene with additions from 1 wt.% to 5 wt.% consolidated into UO2 fuel pellets by spark plasma sintering. The SPS method could avoid traditional powder route mixing and molecular level mixing during the metallurgic process.

5. ACKNOWLEDGEMENTS

The authors express gratitude to the Nuclear and Energy Research Institute (IPEN), National Nuclear Energy Commission (CNEN), and Federal University of Rio de Janeiro (UFRJ).

6. REFERENCES

Acik, M. and Chabal, Y.J., 2011. “Nature of graphene edges: A review.” *Japanese Journal of Applied Physics*, Vol. 50(7R), p. 070101.

Arborelius, J., Backman, K., Hallstadius, L., Limbäck, M., Nilsson, J., Rebensdorff, B., Zhou, G., Kitano, K., Löfström, R. and Rönnberg, G., 2006. “Advanced doped UO_2 pellets in LWR applications.” *Journal of Nuclear Science and Technology*, Vol. 43(9), pp. 967-976.

Bhushan, B., Luo, D., Schricker, S.R., Sigmund, W., Zauscher, S., 2014. Handbook of Nanomaterials Properties, Springer-Verlag Berlin Heidelberg.

Cartas, A., Wang, H., Subhash, G., Baney, R., Tulenko, J., 2015. “Influence of carbon nanotube dispersion in UO_2–Carbon nanotube ceramic matrix composites utilizing spark plasma sintering.” *Nuclear Technology*, Vol. 189(3), pp. 258-267.

Finkeldei, S.C., Kiggans, J.O., Hunt, R. D., Nelson, A.T., Terrani, K A., 2019. “Fabrication of UO_2-Mo composite fuel with enhanced thermal conductivity from sol–gel feedstock.” *Journal of Nuclear Materials*, Vol. 520, pp. 56-64.

Geelhood, K J., Luscher, W.G., Raynaud, P.A., and Porter, I. E., 2015. A Computer Code for the Calculation of Steady-State, Thermal-Mechanical Behavior of Oxide Fuel Rods for High Burnup.

Gomes, D.S., Silva, A.T., 2019. “Performance analysis of UO_2-SiC fuel under normal conditions” In International Nuclear Atlantic Conference (INAC) Santos, SP, pp. 5056-5069.

Gomes, D. S., Muniz, R. O. R. and Giovedi, C., 2017. “Improving performance with accident tolerant fuels” In International Nuclear Atlantic Conference (INAC) Belo Horizonte, MG.

Gomes, D.S., Abe, A., Silva, A.T., Muniz, R.O.R., Giovedi, C. and Martins, M. R., 2019. “Assessment of high conductivity ceramic fuel concept under normal and accident conditions” In Technical Meeting on Modelling of Fuel Behaviour in Design Basis Accidents and Design Extension Conditions, Shenzhen, China.

Hagrman, D.L., Reymann, G.A., 1979. MATPRO-Version 11*: A Handbook of Materials Properties for Use in the Analysis of Light Water Reactor Fuel Rod Behavior* (No. NUREG/CR-0497; TREE-1280). Idaho National Engineering Lab., Idaho Falls USA.

Hilty, F.W. and Tonks, M.R., 2020 “Development and application of a microstructure dependent thermal resistor model for UO_2 reactor fuel with high thermal conductivity additives.*” Journal of Nuclear Materials*, Vol. 540, p. 152334.

Hu, S., Casella, A.M., Lavender, C.A., Senor, D.J., Burkes, D.E., 2015. “Assessment of effective thermal conductivity in U–Mo metallic fuels with distributed gas bubbles.” *Journal of Nuclear Materials*, Vol. 462, pp. 64-76.

Lee, S.W., Kim, H.T. and Bang, I.C., 2011. “Performance of UO_2-Graphene Composite Fuel and SiC Cladding during LOCA.” Transactions of the Korean Nuclear Society Autumn Meeting.

Ironman, T., Tulenko, J. and Subhash, G., 2017. “Exploration of viability of spark plasma sintering for commercial fabrication of nuclear fuel pellets.” *Nuclear Technology*, Vol. 200(2), pp. 144-158.

Kumar, A., Namboodiri, V., Joshi, G., and Mehta, K. P., 2021. Fabrication and applications of fullerene-based metal nanocomposites: A review. *Journal of Materials Research*, Vol. 36(1), pp. 1-15.

Leppänen, J., Pusa, M., Viitanen, T., Valtavirta, V. and Kaltiaisenaho, T., 2015. “The Serpent Monte Carlo code: Status, development, and applications in 2013.” *Annals of Nuclear Energy*, Vol. 82, pp. 142-150.

Porter, I. E. and Geelhood, K. J., 2018. FAST-1.0: A Computer Code for the Calculation of Steady-State and Transient Thermal-Mechanical Behavior of Oxide Fuel Rods.

Subhash, G., Wu, K.H., Tulenko, J., 2014. Development of an Innovative High-Thermal Conductivity UO_2 Ceramic Composites Fuel Pellets with Carbon Nanotubes Using Spark Plasma Sintering (No. 10-917). UT-Battelle LLC/ORNL, Oak Ridge, TN (USA).

Terrani, K.A., 2018. "Accident tolerant fuel cladding development: Promise, status, and challenges." *Journal of Nuclear Materials*, Vol. 501, pp. 13-30.

Terrones, M., Botello-Méndez, A. R., Campos-Delgado, J., López-Urías, F., Vega-Cantú, Y. I., Rodríguez-Macías, F. J., Elías, A. L., Muñoz-Sandoval, E., Cano-Márquez, Charlier, A. G. and Terrones, J.C., 2010. "Graphene and graphite nanoribbons: Morphology, properties, synthesis, defects and applications." *Nano Today*, Vol. 5(4), pp. 351-372.

Tulenko, J. and Subhash, G., 2016. Development of Innovative Accident Tolerant High Thermal Conductivity UO2-Diamond Composite Fuel Pellets (No. DOE/NEUP-12-4037) Univ. of Florida.

Yao, T., Xin, G., Scott, S. M., Gong, B. and Lian, J., 2018. "Thermally conductive and mechanically robust graphene nanoplatelet reinforced UO_2 composite nuclear fuels." *Scientific Reports*, Vol. 8(1), 2987.

Yeo, S., Mckenna, E., Baney, R., Subhash, G. and Tulenko, J., 2013. "Enhanced thermal conductivity of uranium dioxide–silicon carbide composite fuel pellets prepared by Spark Plasma Sintering (SPS)." *Journal of Nuclear Materials*, Vol. 433(1-3), pp. 66-73.

7. RESPONSIBILITY NOTICE

The authors are the only ones responsible for the printed materials included in this article.